

Complex Sparse Signal Recovery with Adaptive Laplace Priors

Zonglong Bai, Liming Shi, Jinwei Sun, and Mads Græsbøll Christensen, *Senior Member, IEEE*

Abstract—Because of its self-regularizing nature and uncertainty estimation, the Bayesian approach has achieved excellent recovery performance across a wide range of sparse signal recovery applications. However, most methods are based on the real-value signal model, with the complex-value signal model rarely considered. Typically, the complex signal model is adopted so that phase information can be utilized. Therefore, it is non-trivial to develop Bayesian models for the complex-value signal model. Motivated by the adaptive least absolute shrinkage and selection operator (LASSO) and the sparse Bayesian learning (SBL) framework, a hierarchical model with adaptive Laplace priors is proposed for applications of complex sparse signal recovery in this paper. The proposed hierarchical Bayesian framework is easy to extend for the case of multiple measurement vectors. Moreover, the space alternating principle is integrated into the algorithm to avoid using the matrix inverse operation. In the experimental section of this work, the proposed algorithm is concerned with both complex Gaussian random dictionaries and directions of arrival (DOA) estimations. The experimental results show that the proposed algorithm offers better sparsity recovery performance than the state-of-the-art methods for different types of complex signals.

Index Terms—Sparse signal recovery, complex sparse signal, sparse Bayesian learning, adaptive Laplace priors.

I. INTRODUCTION

SPARSE signal recovery (SSR) is an active research topic that aims to recover the sparse signal from a set of linear measurements. This is a fundamental problem in signal processing and has practical utility in a wide range of applications. Some applications, such as image processing and electroencephalography (EEG) [1], [2], are based on real-value measurements. In other applications, such as radar signal processing, spectral estimation, blind source separation and magnetic resonance imaging [3]–[5], the complex-value signal model is usually adopted, in which the phase information is also utilized. In reality, the complex-value model is an extension of the real-value model, relying on prior knowledge that the real part and the image part are jointly sparse. Although a complex-value model can be converted into a real-value model, and the real and image parts can be recovered separately [6], [7], nonetheless the joint sparsity of the real and image parts must be further considered. Moreover, the dimensions of the dictionary and measurements are expanded twice, resulting in a higher computational complexity. Thus, we focus on the complex-value signal model in this paper.

Z. Bai and J. Sun are with the School of Instrument Science and Engineering, Harbin Institute of Technology, Harbin, Heilongjiang, 150006 CN e-mail: baizonglong@gmail.com.

L. Shi and M. G. Christensen are with CREATE of Aalborg University, Aalborg, 9000, DK e-mail: {ls, mgc}@create.aau.dk

The least absolute shrinkage and selection operator (LASSO) and its variants have been widely applied to the sparse signal recovery problem [8]–[12]. In [8], the LASSO was proposed for estimation in linear models. The l_1 norm is used as the penalty, which narrows the solution to a finite subset. To deal with the complex-value model, a complex LASSO algorithm was proposed in [9]. The approximate message passing approach is used to ensure the prior knowledge of the joint sparsity. However, the LASSO is not an oracle procedure. To utilize the oracle properties defined in [13], an adaptive LASSO was proposed in [10]. Instead of using a common regularized factor, a series of data-dependent weights are assigned to different coefficients. In the signal processing community, this l_1 norm penalization is also called the basis pursuit. Besides these l_1 norm optimization methods, greedy algorithms are also used for sparse signal recovery and include examples such as the orthogonal matching pursuit [14], [15], greedy pursuit [16], cyclic matching pursuit [17] and subspace pursuit [18].

Both the LASSO methods and the greedy algorithms are the deterministic regularization approach, which provides only a point estimation. Fortunately, the Bayesian framework can also be used to formulate the sparse signal recovery problem. This method is a probabilistic prediction approach that provides both the estimation of model parameters and estimation of uncertainty. In addition, all of the model parameters can be updated automatically when using this method, due to its self-regularizing nature. From a Bayesian perspective, the LASSO is equivalent to building a Bayesian model with Laplace priors [8]. The underlying assumption is that all of the parameters are Laplace-distributed with a common scale factor. However, when considering the conjugate prior principle, the Laplace distribution is not a conjugate prior for the Gaussian distribution. In other words, it is intractable to describe the posterior distribution if Laplace priors are used directly. In [19], a hierarchical Bayesian framework was proposed, called sparse Bayesian learning (SBL). In this hierarchical Bayesian framework, each element of the unknown signal is assigned with an independent zero-mean Gaussian distribution with precision as the hidden parameter. Furthermore, a gamma prior is employed on the parameter of precision as the second stage of the hierarchy. This hierarchical framework is equivalent to adding student-t priors to the likelihood. The student-t prior has similar properties as the Laplace prior, while retaining the conjugacy of the hidden parameter distributions. In this way, the student-t prior is convenient for calculating the posterior distribution of each hidden parameter. In [20], the hierarchical form of Laplace priors was proposed. For the first stage of

the hierarchy, a zero-mean multivariate Gaussian distribution is used to describe the unknown signals, following the SBL framework. For the second stage, independent inverse Gamma priors are assigned to the precision of Gaussian distribution. Considering the marginal distribution with respect to the precision, these first two stages of the hierarchy lead to Laplace priors. Further, a common Gamma prior is assigned to all of the hyper-parameters of the second-stage priors. This hierarchical framework is the Bayesian perspective of LASSO. In [21] and [22], the hierarchical model was improved. Independent Gamma priors are employed to the hyper-parameters of the second-stage hierarchy, which results in a new hierarchical Bayesian model corresponding to the real-value adaptive LASSO.

However, the matrix inverse operation is required for all of the aforementioned Bayesian methods, which leads to a high computational load. To overcome this problem, a basis addition and deletion approach was proposed to accelerate the evidence maximization (type-II maximum likelihood) procedure, which resulted in a faster algorithm [23]. In [20], the criterion of basis addition and deletion was improved for the Laplace priors-based Bayesian model. To the best of the authors knowledge, there is no close form of the criterion for the complex-value signal model. In [24], the space alternative method was used to accelerate the variational Bayesian inference approach. In [25], the space alternative-based method was improved and named the space alternative variational estimation (SAVE) method. In [26], the space alternative method was applied to directions of arrival (DOA) estimation for the multiple measurement vector (MMV) case.

It is worth mentioning that most of the aforementioned methods are based on the real-value signal model. The complex-value signal model is rarely considered either for Bayesian methods or for some of the methods based on convex optimization¹. However, it is necessary to consider the complex problem because the complex-value model is widely used in practice. In this paper, we build a hierarchical Bayesian framework for the complex-value signal model. Inspired by the hierarchical model with Laplace priors proposed in [20] and the adaptive LASSO proposed in [10], we develop a hierarchical Bayesian model with adaptive Laplace priors for the complex-value signal model. The major contributions of this paper are summarized as follows:

- We model complex Laplace priors using a hierarchical Bayesian framework. Using this framework, a hierarchical Bayesian model is built for the complex-value signal, which corresponds to the complex LASSO.
- To meet the oracle properties, the proposed hierarchical model is improved by assigning independent parameters instead of using a common parameter in the second stage of the hierarchy. This hierarchical model corresponds to the complex adaptive LASSO.
- The proposed hierarchical model is built for the single measurement vector (SMV) case. To enhance the general

¹For example, basis pursuit is based on linear programming, but the complex problem cannot be cast as a linear programming problem. Thus, it cannot be directly applied the complex-value signal model.

applicability of the model, we extend it to the MMV case by exploiting the row sparsity of the unknown signal.

- To avoid the matrix inverse operation, the space alternative method is integrated into the proposed method, thereby enhancing the algorithms speed.

The rest of this paper is organized as follows. In the II section, the background of sparse signal recovery is introduced. In the III section, we first give the hierarchical framework of complex Laplace priors. Then, two forms of the hierarchical model, one with complex Laplace priors and the other with complex adaptive Laplace priors, are proposed sequentially. Next, both proposed models are extended to the MMV case. In section IV, the variational Bayesian inference is used to update the hidden parameters of the proposed Bayesian model, and the space alternation method is integrated into the proposed algorithm to avoid the need for a matrix inverse operation. In section V, the performance of the proposed method is tested using complex Gaussian random dictionaries for complex Gaussian signals, complex Laplace signals and complex spike signals. Then, the proposed method is applied to DOA estimation. The conclusion is given in the VI section.

Throughout this paper, the bold symbols in lowercase and uppercase font are reserved for vectors and matrixes, respectively. $\|\cdot\|_p$ and $\|\cdot\|_f$ denote the l_p norm and matrix Frobenius norm, respectively. $(\cdot)^H$ and $(\cdot)^*$ denote the conjugate transpose operation and conjugate operation, respectively. \odot denotes the element product operator. $\text{diag}(\mathbf{v})$ denotes a diagonal matrix with a given vector \mathbf{v} as the diagonal elements. $\mathcal{CN}(\mathbf{x}; \boldsymbol{\mu}, \boldsymbol{\Lambda})$ denotes that the variable \mathbf{x} follows a multivariate normal distribution with the mean $\boldsymbol{\mu}$ and the variance $\boldsymbol{\Lambda}$. $\Gamma(\mathbf{x}; a, b)$ denotes that the variable \mathbf{x} follows a Gamma distribution with the shape parameter a and the rate parameter b . $\Gamma(a)$ denotes a value from the Gamma function. $E_{q(\boldsymbol{\theta})}(\cdot)$ denotes the expectation with the distribution $q(\boldsymbol{\theta})$. \mathbb{C}^M and $\mathbb{C}^{M \times N}$ denote the set of M -dimensional complex vectors and the set of complex matrixes with M rows and N columns, respectively.

II. BACKGROUND AND PROBLEM FORMULATION

In this section, we considered both SMV and MMV cases. For the SMV case, the prior knowledge entails the fact that a few elements of the unknown signals are non-zero while the others are zero. For the MMV case, we assume that a few rows of the unknown signals are non-zero. That is, the unknown signals possess row sparsity for the MMV case.

A. Signal model

1) *Signal model for the SMV case:* Consider the problem of recovering a sparse signal $\mathbf{g} \in \mathbb{C}^N$ from a set of noisy under-sampled linear measurements $\mathbf{x} \in \mathbb{C}^M$ with the observation model as follows:

$$\mathbf{x} = \mathbf{A}\mathbf{g} + \mathbf{w}, \quad (1)$$

where

$$\begin{aligned} \mathbf{x} &= [x_1, \dots, x_m, \dots, x_M]^T, \\ \mathbf{g} &= [g_1, \dots, g_n, \dots, g_N]^T, \\ \mathbf{w} &= [w_1, \dots, w_m, \dots, w_M]^T, \end{aligned}$$

and m is the index of the measurement elements, n is the index of the unknown signal elements, $\mathbf{A} \in \mathbb{C}^{M \times N}$ denotes the dictionary ($M \leq N$), and $\mathbf{w} \in \mathbb{C}^M$ denotes the noise. Given the measurement \mathbf{x} and the dictionary \mathbf{A} , we try to recover the unknown source signal \mathbf{g} as accurately as possible.

2) *Signal model for the MMV case:* Let $\mathbf{X} \in \mathbb{C}^{M \times L}$ represent the MMV and $\mathbf{G} \in \mathbb{C}^{N \times L}$ denote the unknown signal. Then, the observation model for the multi-measurement case can be described as

$$\mathbf{X} = \mathbf{A}\mathbf{G} + \mathbf{W}, \quad (2)$$

where

$$\begin{aligned} \mathbf{X} &= [\mathbf{x}_{\cdot 1}, \dots, \mathbf{x}_{\cdot L}], & \mathbf{x}_{\cdot l} &= [x_{1l}, \dots, x_{Ml}]^T, \\ \mathbf{G} &= [\mathbf{g}_{\cdot 1}, \dots, \mathbf{g}_{\cdot L}], & \mathbf{g}_{\cdot l} &= [g_{1l}, \dots, g_{Nl}]^T, \\ \mathbf{W} &= [\mathbf{w}_{\cdot 1}, \dots, \mathbf{w}_{\cdot L}], & \mathbf{w}_{\cdot l} &= [w_{1l}, \dots, w_{Ml}]^T, \end{aligned}$$

and L is the total number of measurements, while l is the index of the number of measurements.

B. Problem formulation

Considering the under-sampled measurements case, the number of linear measurements M is smaller than the element number of the unknown source signals N . Thus, it is an ill-posed problem to recover either \mathbf{g} or \mathbf{G} using the ordinary least square (OLS) method. To overcome this problem, the minimum power constraint term can be assigned to the OLS, which results in the ridge regression, as follows:

$$\tilde{\mathbf{g}} = \arg \min_{\mathbf{g}} \|\mathbf{x} - \mathbf{A}\mathbf{g}\|_2^2 + \eta \|\mathbf{g}\|_2, \quad (3)$$

where $\tilde{\mathbf{g}}$ denotes the estimation of the unknown signal, while η is a regularized factor. The ridge regression offers a number of computational advantages, although it spreads its energy across all entries instead of a subset. In other words, the ridge regression does not provide a sparse solution.

To exploit the sparse prior knowledge of the unknown signal, a regularized constraint $\|\mathbf{g}\|_0$ is added to the OLS, where the $\|\mathbf{g}\|_0$ norm denotes the number of non-zero elements of \mathbf{g} . This sparse constraint narrows the solution to a finite subset, which results in a more accurate recovery performance than the OLS method. As a result, the sparse signal recovery problem can be described as a minimization optimization problem, as follows:

$$\mathcal{L}(\mathbf{g}) = \arg \min_{\mathbf{g}} \|\mathbf{x} - \mathbf{A}\mathbf{g}\|_2^2 + \eta \|\mathbf{g}\|_0, \quad (4)$$

where η is a predefined regularized factor. However, this optimization problem is intractable because it is an NP-hard problem. The most common way to manage the l_0 -norm is by relaxing it to the l_1 -norm, which results in the following minimization problem:

$$\mathcal{L}(\mathbf{g}) = \arg \min_{\mathbf{g}} \|\mathbf{x} - \mathbf{A}\mathbf{g}\|_2^2 + \eta \|\mathbf{g}\|_1. \quad (5)$$

This estimator can be viewed as an L1-penalized least square estimator, which is also known as a least absolute shrinkage and selection operator, or LASSO [8]. Furthermore, using

a series of data-dependent weights $\boldsymbol{\eta}$ instead of a common weight η , the adaptive LASSO is given as [10]

$$\mathcal{L}(\mathbf{g}) = \arg \min_{\mathbf{g}} \|\mathbf{x} - \mathbf{A}\mathbf{g}\|_2^2 + \mathbf{D} \|\mathbf{g}\|_1, \quad (6)$$

where $\mathbf{D} = \text{diag}(\boldsymbol{\eta})$ is the diagonal weight matrix. Because the adaptive LASSO enjoys the oracle properties, it provides a better basis selection performance than LASSO, which results in an accurate recovery performance [10].

For the MMV case, the prior knowledge includes the fact that the unknown signal has row sparsity. Similar to the SMV case, the adaptive LASSO for the MMV case is

$$\mathcal{L}(\mathbf{G}) = \arg \min_{\mathbf{G}} \|\mathbf{X} - \mathbf{A}\mathbf{G}\|_2^2 + \sum_{i=1}^N \eta_i \|\mathbf{g}_{i\cdot}\|_1, \quad (7)$$

where $\mathbf{g}_{i\cdot}$ denotes the i th row of \mathbf{G} .

The Bayesian representations of (5) and (6) were given in [20] and [21], respectively. Both representations are based on the real-value signal model. To the best of the authors knowledge, the complex-value signal model has not yet been considered. Because there are several differences between the Bayesian frameworks used for the real-value and complex-value signal models, we developed the hierarchical Bayesian model of (5), (6) and (7) for the complex-value signal model in Section III.

III. BAYESIAN MODELING

In Bayesian modeling, all of the unknown variables are treated as stochastic variables. These variables are assigned with different priors, which indicate the prior knowledge of the unknown variables. Motivated by the SBL framework and the hierarchical model of Laplace priors, we propose two Bayesian models for the complex-value signal, i.e., the hierarchical Bayesian model with complex Laplace priors and the hierarchical Bayesian model with complex adaptive Laplace priors. Both the SMV and MMV cases are considered in this section.

A. Single measurement vector case

1) *Noise model:* For the SMV case, we assume that the noise \mathbf{w} is independent complex circular symmetric Gaussian noise with the following distribution:

$$p(\mathbf{w}|\rho) = \mathcal{CN}(\mathbf{w}; \mathbf{0}, \rho^{-1}\mathbf{I}_M), \quad (8)$$

where ρ is the precision of the noise, while \mathbf{I}_M denotes an identity matrix of size M . Based on the observation model (1) and the noise model (8), the likelihood can be described as

$$p(\mathbf{x}|\mathbf{g}, \rho) = \mathcal{CN}(\mathbf{x}; \mathbf{A}\mathbf{g}, \rho^{-1}\mathbf{I}_M). \quad (9)$$

Considering the conjugate prior principle, a Gamma prior is employed for the precision ρ , i.e.,

$$p(\rho|a, b) = \Gamma(\rho; a, b), \quad (10)$$

where $a \geq 0$ is the shape parameter, and $b \geq 0$ is the scale parameter. The mean and variance of ρ are given as $\frac{a}{b}$ and $\frac{a}{b^2}$, respectively.

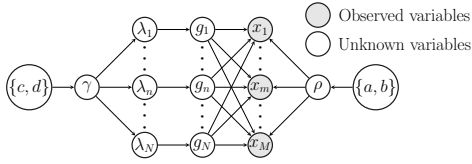


Fig. 1. Directed acyclic graph representation for the hierarchical model with complex Laplace priors (CL-HBM).

2) *Signal model*: To formulate the Bayesian model with Laplace priors, a hierarchical framework is built for the unknown signal. Following the SBL framework, the unknown signal \mathbf{g} is assigned with a zero-mean multivariate complex Gaussian prior as the first-stage, i.e.,

$$p(\mathbf{g}|\boldsymbol{\lambda}) = \mathcal{CN}(\mathbf{g}; \mathbf{0}, \boldsymbol{\Lambda}) = \prod_{i=1}^N \mathcal{CN}(g_i; 0, \lambda_i), \quad (11)$$

where $\boldsymbol{\Lambda}$ is a diagonal matrix with the hyper-parameter $\boldsymbol{\lambda} = [\lambda_1, \dots, \lambda_i, \dots, \lambda_N]$ as the diagonal elements.

In [27] and [20], the real-value model is studied and a Gamma prior is assigned to the parameter $\boldsymbol{\lambda}$ as the second stage of the hierarchy. However, the real-value model cannot be extended to the complex-value model directly. Thus, a new Gamma prior is employed to $\boldsymbol{\lambda}$ for the complex-value signal model, that is

$$p(\boldsymbol{\lambda}|\gamma) = \Gamma(\boldsymbol{\lambda}; \frac{3}{2}, \frac{\gamma}{4}) = \prod_{i=1}^N \Gamma(\lambda_i; \frac{3}{2}, \frac{\gamma}{4}). \quad (12)$$

For the third stage of the hierarchy, a Gamma prior is assigned to γ based on the conjugate prior principle, i.e.,

$$p(\gamma|c, d) = \Gamma(\gamma; c, d). \quad (13)$$

Considering the first two stages of the hierarchy, we have

$$p(\mathbf{g}|\gamma) = \int p(\mathbf{g}|\boldsymbol{\lambda})p(\boldsymbol{\lambda}|\gamma)d\boldsymbol{\lambda} = \frac{\gamma^N}{(2\pi)^N} e^{-\sqrt{\gamma} \sum_{i=1}^N |g_i|}, \quad (14)$$

which is a special case of the complex generalized Gaussian distribution in [28]. In this paper, we treat this case as the complex form of the Laplace prior. Assigning the prior (14) to likelihood (9), the maximum a posteriori (MAP) estimation is equivalent to the l_1 -norm constraint in (5) with the relationship $\eta = \frac{\sqrt{\gamma}}{\rho}$. To the best of the authors knowledge, this work represents the first time that the Gamma prior (12) has been used to form a complex Laplace prior for the complex-value signal (11). The directed acyclic graph of this model is illustrated in Figure 1.

The hierarchical model formed by (9), (10), (11), (12) and (13) corresponds to the complex LASSO. To simplify our description, we call this model the Complex Laplace priors-based Hierarchical Bayesian Model (CL-HBM). Similar to the LASSO, the sparsity of the unknown signal \mathbf{g} is controlled using a common hyper-parameter γ . Thus, this model cannot meet the oracle properties [10]. To overcome this problem, the hierarchical model is improved according to the adaptive LASSO. For the adaptive LASSO, the oracle properties are

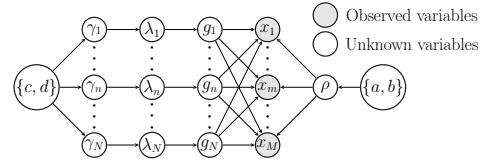


Fig. 2. Directed acyclic graph representation for the hierarchical model with adaptive complex Laplace priors (CAL-HBM).

established by utilizing the adaptively re-weighted l_1 penalty. Therefore, we improve the second stage of the hierarchy as

$$p(\boldsymbol{\lambda}|\gamma) = \Gamma(\boldsymbol{\lambda}; \frac{3}{2}, \frac{\gamma}{4}) = \prod_{i=1}^N \Gamma(\lambda_i; \frac{3}{2}, \frac{\gamma_i}{4}), \quad (15)$$

where $\boldsymbol{\gamma} = [\gamma_1, \dots, \gamma_i, \dots, \gamma_N]$. For the third-stage, a Gamma prior is assigned to the hyper-parameter $\boldsymbol{\gamma}$, i.e.,

$$p(\boldsymbol{\gamma}|c, d) = \Gamma(\boldsymbol{\gamma}; c, d) = \prod_{i=1}^N \Gamma(\gamma_i; c, d). \quad (16)$$

Considering the first-stage Gaussian prior (11) and the new second-stage Gamma prior (15), the marginal distribution $p(\mathbf{g}|\boldsymbol{\gamma})$ obtained by marginalizing the parameter $\boldsymbol{\lambda}$ is

$$p(\mathbf{g}|\boldsymbol{\gamma}) = \int p(\mathbf{g}|\boldsymbol{\lambda})p(\boldsymbol{\lambda}|\boldsymbol{\gamma})d\boldsymbol{\lambda} = \frac{\prod_{i=1}^N \gamma_i}{(2\pi)^N} e^{-\sum_{i=1}^N \sqrt{\gamma_i} |g_i|}. \quad (17)$$

As a result, the hierarchical model formulated by (9), (10), (11), (15) and (16) corresponds to the adaptive LASSO (6) with the relationship $\mathbf{D} = \text{diag}(\rho^{-1} \odot \sqrt{\boldsymbol{\gamma}})$, where $\sqrt{\boldsymbol{\gamma}} = [\sqrt{\gamma_1}, \dots, \sqrt{\gamma_N}]$. Therefore, data-dependent weights are assigned to each element of the unknown signal, observing the oracle properties. In this paper, we call this hierarchical model the Complex Adaptive Laplace prior-based Hierarchical Bayesian Model (CAL-HBM). Figure 2 shows the hierarchical framework of the proposed CAL-HBM.

B. Multiple measurement vector case

According to section III-A, the CAL-HBM is an improvement of the CL-HBM. Thus, in this part, we only give the CAL-HBM for the MMV case, to avoid a duplicate description.

1) *Noise model*: For the MMV case, we assume that the noise is circular symmetric complex Gaussian noise, which is independent owing to its origin from different measurements. Thus, we have

$$p(\mathbf{W}|\rho) = \prod_{l=1}^L p(\mathbf{w}_l|\rho) = \prod_{l=1}^L \mathcal{CN}(\mathbf{w}_l; \mathbf{0}, \rho^{-1} \mathbf{I}_M), \quad (18)$$

where \mathbf{w}_l is the l th column of \mathbf{W} . Next, a Gamma prior is assigned to the noise precision ρ as follows:

$$p(\rho|a, b) = \Gamma(\rho; a, b). \quad (19)$$

Therefore, the likelihood for the MMV case is

$$p(\mathbf{X}|\mathbf{G}, \rho) = \prod_{l=1}^L \mathcal{CN}(\mathbf{x}_l; \mathbf{A}\mathbf{g}_l, \rho^{-1} \mathbf{I}_M), \quad (20)$$

where \mathbf{g}_l is the l 'th column of \mathbf{G} .

2) *Signal model*: Similar to the SMV case, the MMV CAL-HBM is built with a three-stage hierarchical model. We assume that the unknown signal \mathbf{G} has row sparsity, i.e., each row of \mathbf{G} shares a common parameter λ_i that controls the sparsity. Thus, we model each row of \mathbf{G} using a zero-mean multivariate Gaussian distribution, i.e.,

$$p(\mathbf{G}|\boldsymbol{\lambda}) = \prod_{i=1}^N p(\mathbf{g}_i, \lambda_i) = \prod_{i=1}^N \mathcal{CN}(\mathbf{g}_i; \mathbf{0}, \lambda_i \mathbf{I}_L), \quad (21)$$

where \mathbf{g}_i denotes the i th row of \mathbf{G} . For the second stage of the hierarchy, a Gamma prior is assigned to the parameter $\boldsymbol{\lambda}$ as follows:

$$p(\boldsymbol{\lambda}|\boldsymbol{\gamma}) = \prod_{i=1}^N p(\lambda_i|\gamma_i) = \prod_{i=1}^N \Gamma\left(\lambda_i; \frac{1}{2} + L, \frac{\gamma_i}{4}\right). \quad (22)$$

Considering the conjugate prior rule, a Gamma prior is assigned to the parameter $\boldsymbol{\gamma}$ as the third stage, that is

$$p(\boldsymbol{\gamma}|c, d) = \prod_{i=1}^N p(\gamma_i|c, d) = \prod_{i=1}^N \Gamma(\gamma_i; c, d). \quad (23)$$

Similarly, the marginal distribution $p(\mathbf{G}|\boldsymbol{\gamma})$ can be calculated by considering the first two stages of this hierarchy. Thus,

$$\begin{aligned} p(\mathbf{G}|\boldsymbol{\gamma}) &= \int p(\mathbf{G}|\boldsymbol{\lambda})p(\boldsymbol{\lambda}|\boldsymbol{\gamma})d\boldsymbol{\gamma}, \\ &= \int \prod_{i=1}^N \mathcal{CN}(\mathbf{g}_i; \mathbf{0}, \lambda_i \mathbf{I}_L) \Gamma\left(\lambda_i; \frac{1}{2} + L, \frac{\gamma_i}{4}\right) d\boldsymbol{\gamma}, \\ &= \frac{|\boldsymbol{\Lambda}|^L}{\left(4^L \sqrt{\pi} \Gamma\left(\frac{1}{2} + L\right)\right)^N} e^{-\sum_{i=1}^N \sqrt{\gamma_i} (\text{tr}(\mathbf{g}_i \mathbf{g}_i^H))}, \quad (24) \end{aligned}$$

which is a complex Laplace prior. Each row of \mathbf{G} is controlled by a hyper-parameter γ_i . Consequently, the MMV CAL-HBM method is formulated by (20), (19), (21), (22) and (23), which corresponds to the MMV adaptive LASSO (7).

C. Discussion of the proposed models

In this section, we build three hierarchical Bayesian models for the complex-value signal, i.e., the SMV CL-HBM, the SMV CAL-HBM and the MMV CAL-HBM, which correspond to the complex LASSO, the complex adaptive LASSO and the MMV complex adaptive LASSO, respectively. All models are built using a three-layer hierarchical framework. Both the SMV CL-HBM and SMV CAL-HBM methods model the unknown signal using a zero-mean complex Gaussian distribution with independent precision to formulate the first stage of the hierarchy. The difference is that the SMV CAL-HBM assigns independent Gamma priors based on the precision of the Gaussian distribution, which enjoys the oracle properties. The MMV CAL-HBM is a general extension of the SMV CAL-HBM. In other words, the SMV CAL-HBM is a special case of the MMV CAL-HBM when the number of measurements $L = 1$.

IV. VARIATIONAL BAYESIAN INFERENCE

Thus far, we have presented the proposed CAL-HBM. In this section, the variational Bayesian inference is used to calculate all hidden parameters of CAL-HBM. Moreover, the space alternative method is utilized to avoid the matrix inverse operation. For the convenience of comprehension, the derivation of the SMV case is given first. Then, the MMV case is given as an extension of the SMV case.

A. Variational Bayesian inference

In variational Bayesian inference, the true posterior distribution $p(\boldsymbol{\theta}|\mathbf{x})$ is approximated by a distribution $q(\boldsymbol{\theta})$, which has a factorized form as follows:

$$q(\boldsymbol{\theta}) = q_g(\mathbf{g})q_\lambda(\boldsymbol{\lambda})q_\gamma(\boldsymbol{\gamma})q_\rho(\rho), \quad (25)$$

where $\boldsymbol{\theta} = \{\mathbf{g}, \boldsymbol{\lambda}, \boldsymbol{\gamma}, \rho\}$ is the set of all unknown parameters.

The logarithmic evidence $\ln p(\mathbf{x})$ can be written as

$$\ln p(\mathbf{x}) = \int q(\boldsymbol{\theta}) \ln \frac{p(\mathbf{x}, \boldsymbol{\theta})}{q(\boldsymbol{\theta})} d\boldsymbol{\theta} + \int q(\boldsymbol{\theta}) \ln \frac{q(\boldsymbol{\theta})}{p(\boldsymbol{\theta}|\mathbf{x})} d\boldsymbol{\theta}. \quad (26)$$

The first and second terms on the right side of (26) are the evidence lower bound \mathcal{L} and the KullbackLeibler (KL) divergence \mathcal{K} , respectively, i.e.,

$$\mathcal{L} = \int q(\boldsymbol{\theta}) \ln \frac{p(\mathbf{x}, \boldsymbol{\theta})}{q(\boldsymbol{\theta})} d\boldsymbol{\theta}, \quad \mathcal{K} = \int q(\boldsymbol{\theta}) \ln \frac{q(\boldsymbol{\theta})}{p(\boldsymbol{\theta}|\mathbf{x})} d\boldsymbol{\theta}.$$

The parameters of the approximate distribution $q(\boldsymbol{\theta})$ are calculated by minimizing the KL divergence \mathcal{K} . Because the evidence $p(\mathbf{x})$ is a constant and $\mathcal{K} \geq 0$, minimizing the KL divergence is equivalent to maximizing the lower bound \mathcal{L} , which results in [29]

$$\ln q(\boldsymbol{\theta}_k) = E_{q(\boldsymbol{\theta} \setminus \boldsymbol{\theta}_k)} (\ln p(\mathbf{x}, \boldsymbol{\theta})) + \text{cons}, \quad (27)$$

$$p(\mathbf{x}, \boldsymbol{\theta}) = p(\mathbf{x}|\mathbf{g}, \rho)p(\mathbf{g}|\boldsymbol{\lambda})p(\boldsymbol{\lambda}|\boldsymbol{\gamma})p(\boldsymbol{\gamma})p(\rho), \quad (28)$$

where cons denotes a constant, $\boldsymbol{\theta}_k$ denotes a subset of $\boldsymbol{\theta}$, and $\boldsymbol{\theta} \setminus \boldsymbol{\theta}_k$ denotes the subset of $\boldsymbol{\theta}$ with $\boldsymbol{\theta}_k$ pruned.

B. Single measurement vector case

Substituting the likelihood (9), the Gamma prior of noise precision (10), the model of the unknown signal (11), (15) and (16) into (28), the joint distribution can be written as follows:

$$\begin{aligned} \ln p(\mathbf{x}, \boldsymbol{\theta}) &= M \ln \rho - \rho \|\mathbf{x} - \mathbf{A}\mathbf{g}\|^2 + \sum_{i=1}^N \ln \lambda_i^{-1} - \\ &\quad \mathbf{g}^H \boldsymbol{\Lambda}^{-1} \mathbf{g} + \frac{3}{2} \sum_{i=1}^N \ln \gamma_i + \frac{1}{2} \sum_{i=1}^N \ln \lambda_i - \\ &\quad \frac{1}{4} \sum_{i=1}^N \gamma_i \lambda_i + \sum_{i=1}^N (c-1) \ln \gamma_i - \sum_{i=1}^N d\gamma_i + \\ &\quad (a-1) \ln \rho - b\rho + c_x, \quad (29) \end{aligned}$$

where c_x denotes the normalization factor constant of the joint distribution. In the following derivation, c_g , c_{λ_i} , c_{γ_i} and c_{rho} denote the normalization factor constant of each distribution, respectively. Given the form of joint distribution, all of the parameters can be updated using (27) and (28), as shown in the following.

1) *Update of $q_g(\mathbf{g})$* : According to (27), the variational approximation of $\ln p(\mathbf{g}|\mathbf{x})$ is

$$\begin{aligned} \ln q(\mathbf{g}) &= \mathbb{E}_{q(\boldsymbol{\theta}|\mathbf{g})}(\ln p(\mathbf{x}, \boldsymbol{\theta})), \\ &= -\mathbf{g}^H \left(\rho \mathbf{A}^H \mathbf{A} + \boldsymbol{\Lambda}^{-1} \right) \mathbf{g} + \rho \mathbf{g}^H \mathbf{A}^H \mathbf{x} + \\ &\quad \rho \mathbf{x}^H \mathbf{A} \mathbf{g} - \rho \mathbf{x}^H \mathbf{x} + c_g, \end{aligned} \quad (30)$$

which indicates that $q(\mathbf{g})$ can be described using a multivariate complex Gaussian distribution with the mean and variance given as

$$\begin{aligned} \boldsymbol{\mu}_g &= \mathbb{E}_{q(\rho)}(\rho) \boldsymbol{\Sigma} \mathbf{A}^H \mathbf{x}, \\ \boldsymbol{\Sigma}_g &= \left(\mathbb{E}_{q(\rho)}(\rho) \mathbf{A}^H \mathbf{A} + \mathbb{E}_{q(\boldsymbol{\Lambda})}(\boldsymbol{\Lambda}^{-1}) \right)^{-1}. \end{aligned} \quad (31)$$

Therefore, we have the updated rule for \mathbf{g} given as

$$\mathbb{E}_{q(\mathbf{g})}(\mathbf{g}) = \mathbb{E}_{q(\rho)}(\rho) \boldsymbol{\Sigma} \mathbf{A}^H \mathbf{x}. \quad (32)$$

2) *Update of $q_\lambda(\boldsymbol{\lambda})$, $q_\gamma(\boldsymbol{\gamma})$ and $q_\rho(\rho)$* : See Appendix A

The unknown parameters can be updated using (32), (43), (44), (46) and (47), iteratively. However, the matrix inverse operation is required in (32), which entails a heavy computational load. To reduce the computational complexity, the space alternative principle is used in the variational Bayesian inference, as detailed in the following.

3) *Space alternative variational estimation*: If we assume that each element of \mathbf{g} is independent and the approximate posterior $q(\mathbf{g})$ can be factorized, then we have $q(\mathbf{g}) = \prod_{i=1}^N q(g_i)$. Thus, the approximate posterior of g_i can be derived from (27). That is,

$$\begin{aligned} \ln q(g_i) &= \mathbb{E}_{q(\boldsymbol{\theta}|\mathbf{g}_i)}(\ln p(\mathbf{x}, \boldsymbol{\theta})), \\ &= g_i^H \left(\mathbb{E}_{q(\rho)}(\rho) \mathbf{A}_i^H \mathbf{A}_i + \mathbb{E}_{q(\lambda_i)}(\lambda_i^{-1}) \right) g_i - \\ &\quad \mathbb{E}_{q(\rho)}(\rho) g_i^H \mathbf{A}_i^H \left(\mathbf{x} - \mathbf{A}_{\bar{i}} \mathbb{E}_{q(\mathbf{g}_{\bar{i}})}(\mathbf{g}_{\bar{i}}) \right) - \\ &\quad \mathbb{E}_{q(\rho)}(\rho) \left(\mathbf{x} - \mathbf{A}_{\bar{i}} \mathbb{E}_{q(\mathbf{g}_{\bar{i}})}(\mathbf{g}_{\bar{i}}) \right)^H \mathbf{A}_i g_i + c_{g_i}, \end{aligned} \quad (33)$$

where \mathbf{A}_i denotes the i th column of the dictionary, g_i denotes the i th element of the vector \mathbf{g} , $\mathbf{A}_{\bar{i}}$ denotes the dictionary with the i th column pruned, and $\mathbf{g}_{\bar{i}}$ denotes the vector with the i th element pruned. Note that an equality formulation is used in (33), i.e.,

$$\mathbf{A} \mathbf{x} = \mathbf{A}_i g_i + \mathbf{A}_{\bar{i}} \mathbf{g}_{\bar{i}}.$$

Considering the quadratic form of (33), a complex Gaussian distribution can be used to represent the approximate posterior $q(g_i)$ with the following parameters:

$$\sigma_i^2 = \frac{1}{\mathbb{E}_{q(\rho)}(\rho) \mathbf{A}_i^H \mathbf{A}_i + \mathbb{E}_{q(\lambda_i)}(\lambda_i^{-1})}, \quad (34)$$

$$\boldsymbol{\mu}_i = \sigma_i^2 \mathbb{E}_{q(\rho)}(\rho) \mathbf{A}_i^H \left(\mathbf{x} - \mathbf{A}_{\bar{i}} \mathbb{E}_{q(\mathbf{g}_{\bar{i}})}(\mathbf{g}_{\bar{i}}) \right). \quad (35)$$

Thus, the update rule of g_i is

$$\mathbb{E}_{q(g_i)} = \sigma_i^2 \mathbb{E}_{q(\rho)}(\rho) \mathbf{A}_i^H \left(\mathbf{x} - \mathbf{A}_{\bar{i}} \mathbb{E}_{q(\mathbf{g}_{\bar{i}})}(\mathbf{g}_{\bar{i}}) \right). \quad (36)$$

In this way, the parameters of CAL-HBM are calculated using the space alternative variational estimation algorithm, which updates the unknown parameters using (35), (43), (44), (46) and (47), iteratively. For simplicity, we call the proposed algorithm CAL-SAVE.

C. Multiple measurement vector case

Similar to the SMV case, the joint distribution $p(\mathbf{X}, \mathbf{G}, \boldsymbol{\lambda}, \boldsymbol{\gamma}, \rho)$ can be represented using the likelihood (20), the Gamma prior of noise precision (19), the model of the unknown signal (21), (22) and (23). As a result, we obtain

$$\begin{aligned} \ln p(\mathbf{X}, \boldsymbol{\theta}) &= \ln (p(\mathbf{X}|\mathbf{G}, \rho) p(\mathbf{G}|\boldsymbol{\lambda}) p(\boldsymbol{\lambda}|\boldsymbol{\gamma}) p(\boldsymbol{\gamma}|c, d) p(\rho|a, b)), \\ &= LM \ln \rho - \rho \|\mathbf{X} - \mathbf{A} \mathbf{G}\|_F^2 + L \sum_{i=1}^N \ln \lambda_i^{-1} - \\ &\quad \sum_{i=1}^N \lambda_i^{-1} \text{tr}(\mathbf{g}_i^H \mathbf{g}_i) + \left(\frac{1}{2} + L \right) \sum_{i=1}^N \ln \gamma_i + (L - \frac{1}{2}) \sum_{i=1}^N \ln \lambda_i - \\ &\quad \frac{1}{4} \sum_{i=1}^N \gamma_i \lambda_i + (c-1) \sum_{i=1}^N \ln \gamma_i - d \sum_{i=1}^N \gamma_i + (a-1) \ln \rho - \\ &\quad b\rho + c_X, \end{aligned} \quad (37)$$

where c_X is a constant of the normalized factor. In the following, c_G , c_λ , c_γ and c_ρ represent the constants of the normalized factor for the MMV case.

1) *Update of $q(\mathbf{g}_i)$* : Because we assume that the unknown signal \mathbf{G} has row sparsity, each row can be processed independently using the SAVE algorithm. According to (27) and (37), the approximate posterior of \mathbf{g}_i is

$$\begin{aligned} \ln q(\mathbf{g}_i) &= \ln \mathbb{E}_{q(\boldsymbol{\theta}|\mathbf{g}_i)}(p(\mathbf{X}, \boldsymbol{\theta})), \\ &= -\text{tr} \left(\mathbf{g}_i^H (\mathbb{E}_{q(\rho)}(\rho) \mathbf{A}_i^H \mathbf{A}_i + \mathbb{E}_{q(\lambda_i)}(\lambda_i^{-1})) \mathbf{g}_i + \right. \\ &\quad \mathbb{E}_{q(\rho)}(\rho) \mathbf{g}_i^H \mathbf{A}_i^H (\mathbf{X} - \mathbf{A}_{\bar{i}} \mathbb{E}_{q(\mathbf{g}_{\bar{i}})}(\mathbf{g}_{\bar{i}})) + \\ &\quad \left. \mathbb{E}_{q(\rho)}(\rho) (\mathbf{X} - \mathbf{A}_{\bar{i}} \mathbb{E}_{q(\mathbf{g}_{\bar{i}})}(\mathbf{g}_{\bar{i}}))^H \mathbf{A}_i \mathbf{g}_i \right) + c_G, \end{aligned}$$

where \mathbf{g}_i denotes the i th row of the signal \mathbf{G} , and $\mathbf{g}_{\bar{i}}$ denotes the signal with the i th row pruned. The multivariate quadratic form of $\ln q(\mathbf{g}_i)$ indicates that the approximate distribution $q(\mathbf{g}_i)$ can be described using a multivariate complex Gaussian distribution with parameters given as

$$\sigma_i^2 = \frac{1}{\mathbb{E}_{q(\rho)}(\rho) \mathbf{A}_i^H \mathbf{A}_i + \mathbb{E}_{q(\lambda_i)}(\lambda_i^{-1})}, \quad (38)$$

$$\boldsymbol{\mu}_i = \sigma_i^2 \mathbb{E}_{q(\rho)}(\rho) \mathbf{A}_i^H (\mathbf{X} - \mathbf{A}_{\bar{i}} \mathbb{E}_{q(\mathbf{g}_{\bar{i}})}(\mathbf{g}_{\bar{i}})). \quad (39)$$

Therefore, \mathbf{g}_i is updated using

$$\mathbb{E}_{q(\mathbf{g}_i)}(\mathbf{g}_i) = \sigma_i^2 \mathbb{E}_{q(\rho)}(\rho) \mathbf{A}_i^H (\mathbf{X} - \mathbf{A}_{\bar{i}} \mathbb{E}_{q(\mathbf{g}_{\bar{i}})}(\mathbf{g}_{\bar{i}})). \quad (40)$$

2) *Update of $q_\lambda(\boldsymbol{\lambda})$, $q_\gamma(\boldsymbol{\gamma})$ and $q_\rho(\rho)$* : See Appendix B

All of the hidden parameters are updated using (40), (48), (49), (50) and (51), sequentially. The proposed algorithm for the MMV case is summarized in Algorithm 1².

²To avoid duplicate calculation, a temporary variable \mathbf{X}_{tmp} is used in the algorithm. Note that the SMV CAL-SAVE is a special case of the MMV CAL-SAVE, where the number of measurement vectors is 1.

Algorithm 1: An overview of the proposed algorithms

Input: The MMV data \mathbf{X} , the dictionary \mathbf{A} , and the prior parameters a, b, c and d .

Output: The recovered source signals \mathbf{G} and the variance σ^2

Initialize the precision of noise $\rho = \frac{a}{b}$;

Initialize the hyper-parameter $\gamma_i = \frac{c}{d}$, $\gamma_i^{-1} = \frac{d}{c}$, and $\lambda_i = \frac{b}{\gamma_i}$, for $i = 1, \dots, N$;

Initialize the mean of the variable $\mathbf{G} = \mathbf{0}$ and the variance of the variable $\sigma_i^2 = \frac{1}{\rho \mathbf{A}_i^H \mathbf{A}_i + \lambda_i^{-1}}$, for $i = 1, \dots, N$;

Initialize the temporary variable $\mathbf{X}_{\text{tmp}} = \mathbf{A}\mathbf{G}$;

while convergence criterion not met **do**

for $i \leftarrow 1$ **to** N **do**

 Update $\mathbf{g}_i^{\text{old}} \leftarrow \mathbf{g}_i$;

 Update $\mathbf{X}_{\text{tmp}} \leftarrow \mathbf{X}_{\text{tmp}} - \mathbf{A}_i \mathbf{g}_i^{\text{old}}$;

 Update $\sigma_i^2 \leftarrow \frac{1}{\rho \mathbf{A}_i^H \mathbf{A}_i + \gamma_i^{-1}}$ using (38);

 Update $\mathbf{g}_i \leftarrow \sigma_i^2 \rho \mathbf{A}_i^H (\mathbf{X} - \mathbf{X}_{\text{tmp}})$ using (40);

 Update $\mathbf{X}_{\text{tmp}} \leftarrow \mathbf{X}_{\text{tmp}} + \mathbf{A}_i \mathbf{g}_i$;

 Update $\lambda_i \leftarrow 2 \left(\frac{\sqrt{\text{tr}(\mathbf{g}_i^H \mathbf{g}_i) + \sigma_i^2}}{\sqrt{\gamma_i}} + \frac{1}{\gamma_i} \right)$ using (48);

 Update $\lambda_i^{-1} \leftarrow \frac{1}{\lambda_i - \frac{2}{\gamma_i}}$ using (49);

 Update $\gamma_i \leftarrow \frac{4(L+c)+2}{\lambda_i + 4d}$ using (50);

end

 Update $\rho \leftarrow \frac{LM+a}{\|\mathbf{X} - \mathbf{A}\mathbf{E}_q(\mathbf{G})\|^2 + \sum_{i=1}^N \sigma_i^2 \mathbf{A}_i^H \mathbf{A}_i + b}$ based

 on (51);

end

V. EXPERIMENTAL RESULTS

In this section, we first test the recovery accuracy of the different algorithms with complex Gaussian random dictionaries. Then, the proposed algorithms are applied to DOA estimation featuring a deterministic dictionary. We compare the performance of the proposed method with other state-of-the-art methods that are widely used in sparse signal recovery. All methods in the comparison are summarized as follows:

- ‘CAL-SAVE’ refers to the proposed method based on the hierarchical Bayesian model with complex adaptive Laplace priors³.
- ‘CL-SAVE’ refers to the proposed method based on the hierarchical model with complex Laplace priors.
- ‘FLap-Real’ is a Laplace signal model-based fast method that uses the basis addition and deletion proposed in [20].
- ‘SAVE-SBL’ is the SAVE-based SBL algorithm proposed in [25]. We improve this algorithm for the complex-value signal model.
- ‘LASSO’ refers to the LASSO method that uses the complex-value signal model [8].
- ‘MFOCUSS’ refers to the focal underdetermined system solver proposed in [30]. Following the setup in this paper, the parameter p is set to 0.8.

- ‘SBL-BF’ is a complex signal recovery method that uses SBL and the beamforming method, as proposed in [31].
- ‘CSMUSIC’ is a subspace pursuit method for sparse signal recovery, as proposed in [18].

A. Experiment using complex Gaussian random dictionaries

To quantify the sparse recovery performance of the different algorithms, the root mean square error criteria are used, defined as

$$e_{\text{RMSE}} = \frac{\sqrt{\sum_{n=1}^{N_{MC}} \|\tilde{\mathbf{G}}^n - \mathbf{G}^n\|_f^2}}{KN_{MC}}, \quad (41)$$

where n and N_{MC} are the index and total numbers of Monte-Carlo experiments, respectively. K is the total number of elements of \mathbf{G} . $\tilde{\mathbf{G}}^n$ and \mathbf{G}^n are the estimation and the truth values of the n th Monte-Carlo experiments, respectively.

1) *Experimental setup:* We test the performance of all methods under different scenarios, including different SNR, sparsity, and length of measurement vectors. For each case, three types of signal are used for testing, i.e., a complex Gaussian signal, complex Laplace signal and complex spike signal. The real and image parts of these signals are generated independently following the same distribution with a common variance. The dictionaries are built by sampling from a normal distribution, i.e., $\Re(a_{i,j}) \sim \mathcal{N}(0, 1)$ and $\Im(a_{i,j}) \sim \mathcal{N}(0, 1)$ and are normalized for each row. The index of non-zero elements is selected randomly. The prior parameters a, b, c and d are set to a small value 10^{-4} . For all of the cases, the number of Monte-Carlo experiments is set to 1000. We test the performance for the SMV and MMV cases, in order.

The setup for the SMV case is summarized as follows:

- In the first experiment, the performance of the different methods is tested for three types of signals under various lengths of the measurement vector, which ranges from 50 to 150 with an interval of 10. The length of signal N is fixed to 200 while the number of non-zero elements is set to 20. The SNR is set to 10 dB.
- In the second experiment, the recovery performance for different types of signals under different sparsity values is tested. The length of the signal is fixed to 200, while the number of non-zero elements is changed from 5 to 30 with an interval of 5. The length of the measurements is fixed to 100. The SNR is set to 10 dB.
- In the third experiment, we test the performance of the different methods for three types of signals under complex white Gaussian noise. The SNRs ranged from 0 dB to 30 dB with an interval of 5 dB. The length of the measurement vector is set to $M = 100$. The length of the unknown signal is set to $N = 200$, and the number of non-zero elements is set to $K = 20$.

For the MMV case, the hyper-prior parameters a, b, c and d are set to 10^{-6} . In the first experiments, the recovery performance is tested for different types of signals under different numbers of measurement vectors in the range of 1 to 10 with an interval of 1. The length of the measurement vectors is fixed to 100. The number of signal elements is fixed to 200,

³The MATLAB code for the proposed algorithm is available online: <https://tinyurl.com/ub5jroa>.

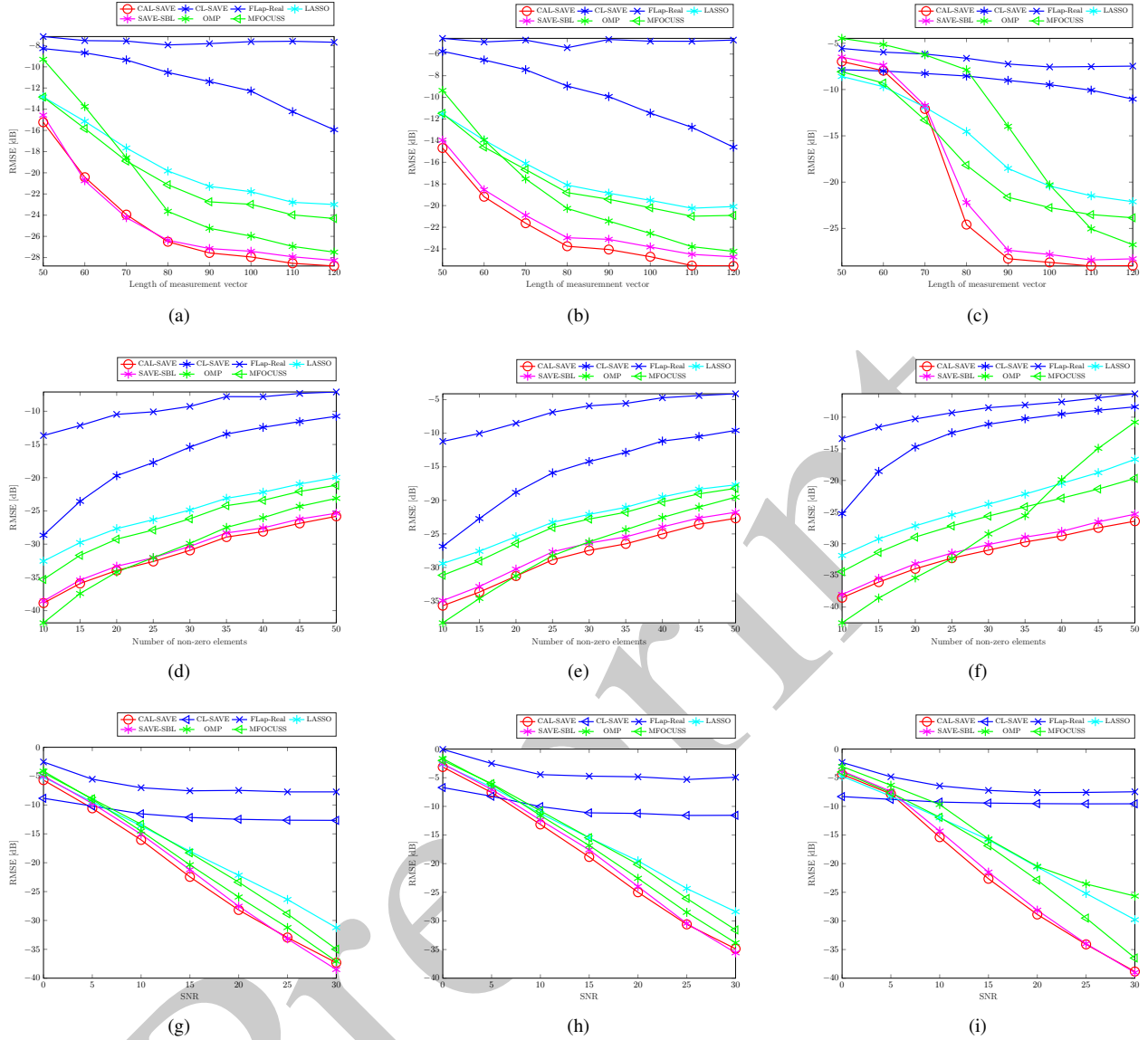


Fig. 3. Simulation results for the SMV case with the complex Gaussian random dictionaries. (a) RMSE for the Gaussian signal versus the number of measurement vectors, (b) RMSE for the Laplace signal versus the number of measurement vectors, (c) RMSE for the spike signal versus the number of measurement vectors, (d) RMSE for the Gaussian signal versus the sparsity, (e) RMSE for the Laplace signal versus the sparsity, (f) RMSE for the spike signal versus the sparsity, (g) RMSE for the Gaussian signal versus the SNR, (h) RMSE for the Laplace signal versus the SNR, (i) RMSE for the spike signal versus the SNR.

while the number of non-zero elements is set to 40. The SNR is set to 10 dB. In the following three experiments, we test the recovery performance for different measurements, SNR and sparsity, similar to the SMV case. The setup is identical to the SMV case except that the number of snapshots is set to 5.

2) *Performance analysis for the SMV case:* Figure 3a, Figure 3b and Figure 3c show the recovery accuracy of each algorithm versus the number of measurements for the complex Gaussian signal, complex Laplace signal and complex spike signal, respectively. It can be seen that ‘SAVE-SBL’ and the proposed ‘CAL-SAVE’ achieve the best performance of these three cases. The difference between ‘SAVE-SBL’ and the proposed algorithm is that the former models the signal using a complex Gaussian prior, whereas the latter uses a complex

Laplace prior to model the signal. These two models have similar recovery performance for the complex Gaussian signal. However, for the Laplace signal, the proposed ‘CAL-SAVE’ method achieves better performance than ‘SAVE-SBL’. The reason for this result is that the complex Laplace prior gives a better description of complex Laplace signals. In other words, the statistics hypothesis matches the signal model. Besides, for the spike signal, the proposed ‘CAL-SAVE’ method achieves better performance than either the ‘SAVE-SBL’ method or the other methods. In contrast to the ‘CAL-SAVE’ method and ‘SAVE-SBL’ method, both the ‘CL-SAVE’ and ‘FLap’ methods are assigned with a common Gamma prior. The difference between the models is that ‘CL-SAVE’ is derived from the variational Bayesian inference, whereas ‘FLap’ is based on evidence maximization (type-II maximum likelihood)

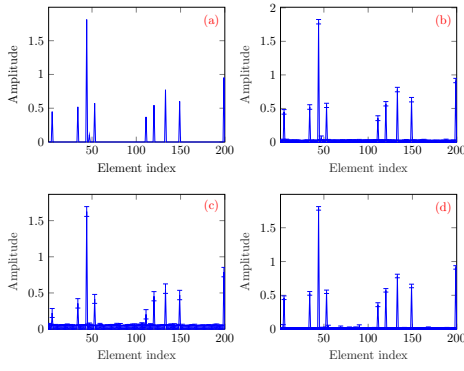


Fig. 4. The standard deviation of different methods for Gaussian signals. (a) Original Signal. (b) CAL-SAVE. (c) CL-SAVE. (d) SAVE-SBL.

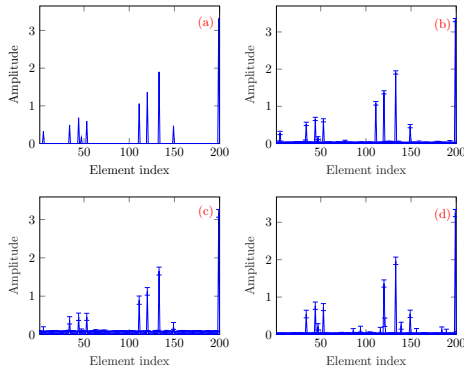


Fig. 5. The standard deviation of different methods for Laplace signals. (a) Original Signal. (b) CAL-SAVE. (c) CL-SAVE. (d) SAVE-SBL.

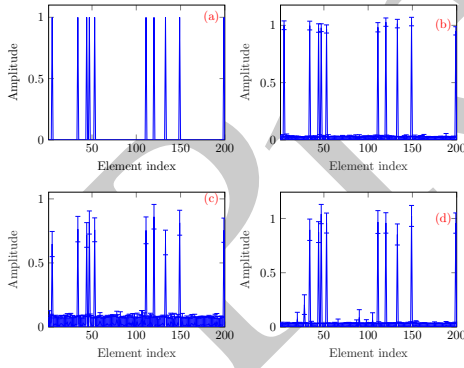


Fig. 6. The standard deviation of different methods for spike signals. (a) Original Signal. (b) CAL-SAVE. (c) CL-SAVE. (d) SAVE-SBL.

[32]. Because no method has been reported that entails both basis addition and deletion for the complex-value model, the 'FLap' method is implemented based on the real-value model. Furthermore, because the model with a common prior does not meet the oracle properties [10], these two methods exhibit worse performance results than the others.

The recovery performances under different sparsity levels for the complex Gaussian signal, complex Laplace signal and complex spike signal are illustrated in Figure 3d, Figure 3e and Figure 3f, respectively. As can be seen from these figures, with a decreasing sparsity level, the performance of

all methods is degraded. Note that the sparsity is known for the OMP algorithm. Thus, this method achieves a better recovery performance than the other methods in the range from 10 to 20. However, the proposed 'CAL-SAVE' outperforms the other methods when the number of non-zero elements is larger than 20, even without prior knowledge of the sparsity level.

Figure 3g, Figure 3h and Figure 3i show the recovery performance under different SNRs for the complex Gaussian signal, complex Laplace signal and complex spike signal, respectively. The performance of all methods is improved as the SNR increases. In comparison with other state-of-the-art methods, the proposed 'CAL-SAVE' method has the best recovery performance in the SNR range from 5 to 20 dB.

In comparison with the LASSO and the adaptive LASSO, the Bayesian methods provide the uncertainty of estimation using the variance of the posterior distributions. In this part, the uncertainty values of three Bayesian methods, i.e., 'CAL-SAVE', 'CL-SAVE' and 'SAVE-SBL', are compared. We consider the SMV case. The length of the measurement vector is 100. The length of the signals is 200, while the number of non-zero elements is 10. The SNR is set to 10 dB. Figure 4, Figure 5 and Figure 6 illustrate the uncertainty of estimations for the complex Gaussian signal, complex Laplace signal and complex spike signal, respectively. The error bars are labeled using one standard derivation, σ_i . As can be seen in these figures, the 'SAVE-SBL' and the proposed 'CAL-SAVE' methods have smaller variances than the 'CL-SAVE' method for all of the signal types. The main reason for this result is that the 'SAVE-SBL' and 'CAL-SAVE' methods meet the oracle properties, whereas the 'CL-SAVE' method does not. Comparing the 'CAL-SAVE' method with 'SAVE-SBL', it can be seen that 'CAL-SAVE' achieves a better recovery accuracy than 'SAVE-SBL', which is identical to the result indicated in Figure 3.

3) *Performance for the MMV case:* In the first experiments of the MMV case, the recovery performance of different methods is tested under different numbers of measurement vectors, as shown in Figure 7a, Figure 7b and Figure 7c. From these figures, it can be seen that using a larger number of measurement vectors leads to a better recovery performance. For the 'SBL-BF' and 'CSMUSIC' methods, we assume that the sparsity is known. Thus, the performance of these methods is better than that of the others when $L = 1$. In comparison with the 'SBL-BF' and 'CSMUSIC' methods, the 'SAVE-SBL' and 'CAL-SAVE' methods do not require prior knowledge of the sparsity level but do achieve a better recovery performance than other state-of-the-art methods when the number of snapshots is greater than 1.

Figure 7d, Figure 7e and Figure 7f show the recovery performance under different lengths of measurement vectors for the complex Gaussian signal, complex Laplace signal and complex spike signal, respectively. Similar to the SMV case, longer measurements lead to better recovery performances. As can be seen from these figures, the proposed method, which lacks prior knowledge of the sparsity level, achieves a better performance than the 'MFOCUSS', 'SBL-BF' and 'CSMUSIC' methods in most of the scenarios.

The recovery performance under different SNRs for the

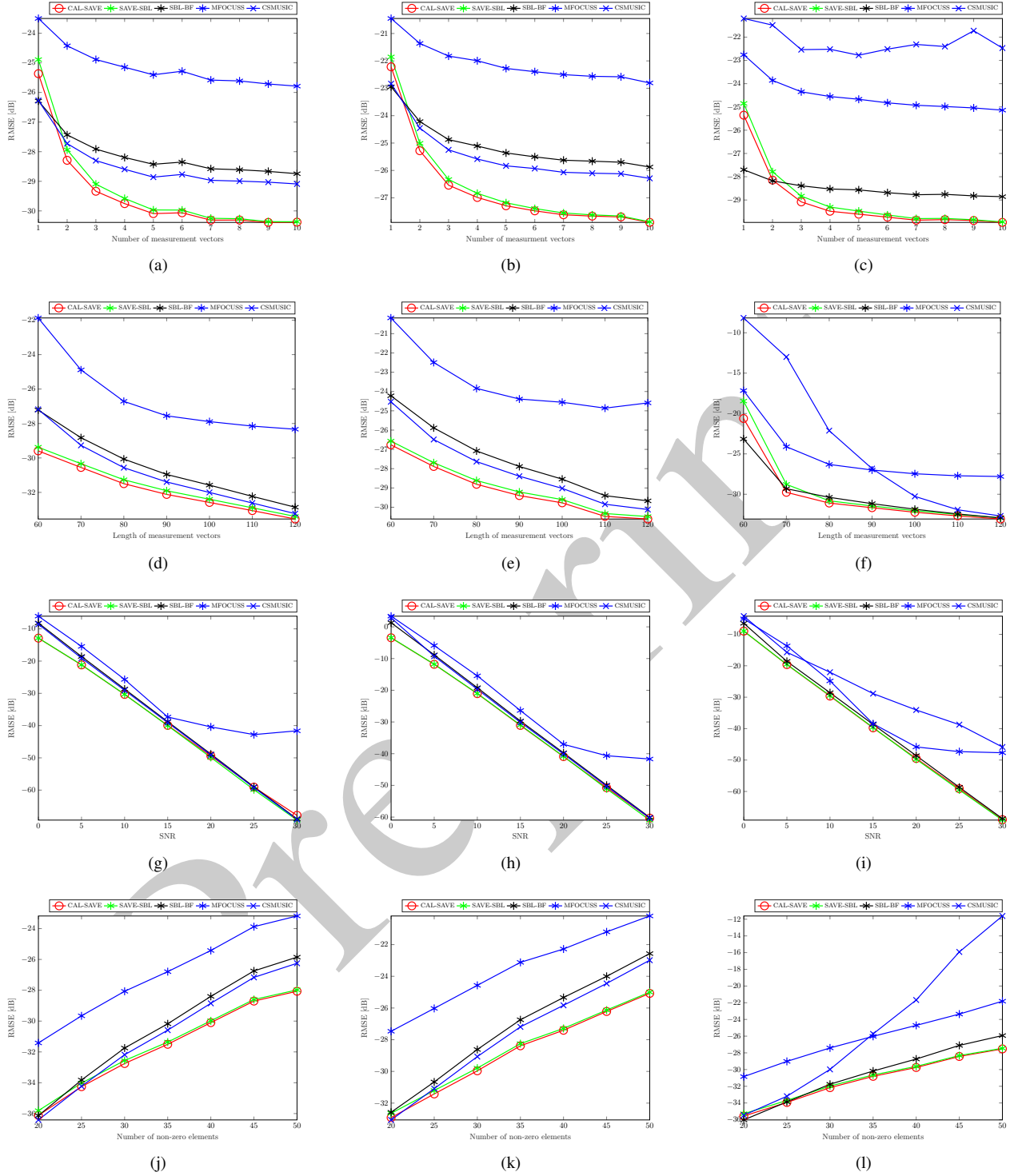


Fig. 7. Simulation results for the MMV case with the complex Gaussian random dictionaries. (a) RMSE versus the number of measurements for the Gaussian signal, (b) RMSE versus the number of measurements for the Laplace signal, (c) RMSE versus the number of measurements for the spike signal, (d) RMSE versus the sparsity for the Gaussian signal, (e) RMSE versus the sparsity for the Laplace signal, (f) RMSE versus the sparsity for the spike signal, (g) RMSE versus the SNR for the Gaussian signal, (h) RMSE versus the SNR for the Laplace signal, (i) RMSE versus the SNR for the spike signal.

complex Gaussian signal, complex Laplace signal and complex spike signal is tested in the third experiment, as shown in Figure 7g, Figure 7h and Figure 7i, respectively. Both the proposed method ‘CAL-SAVE’ and ‘SAVE-SBL’ are based on the hierarchical Bayesian model. As a result, these methods

outperform the others in the range from 0 dB to 20 dB.

Figure 7j, Figure 7k and Figure 7l show the performance under different sparsity values for the complex Gaussian signal, complex Laplace signal and complex spike signal, respectively. Both the ‘SBL-BF’ and ‘CSMUSIC’ methods

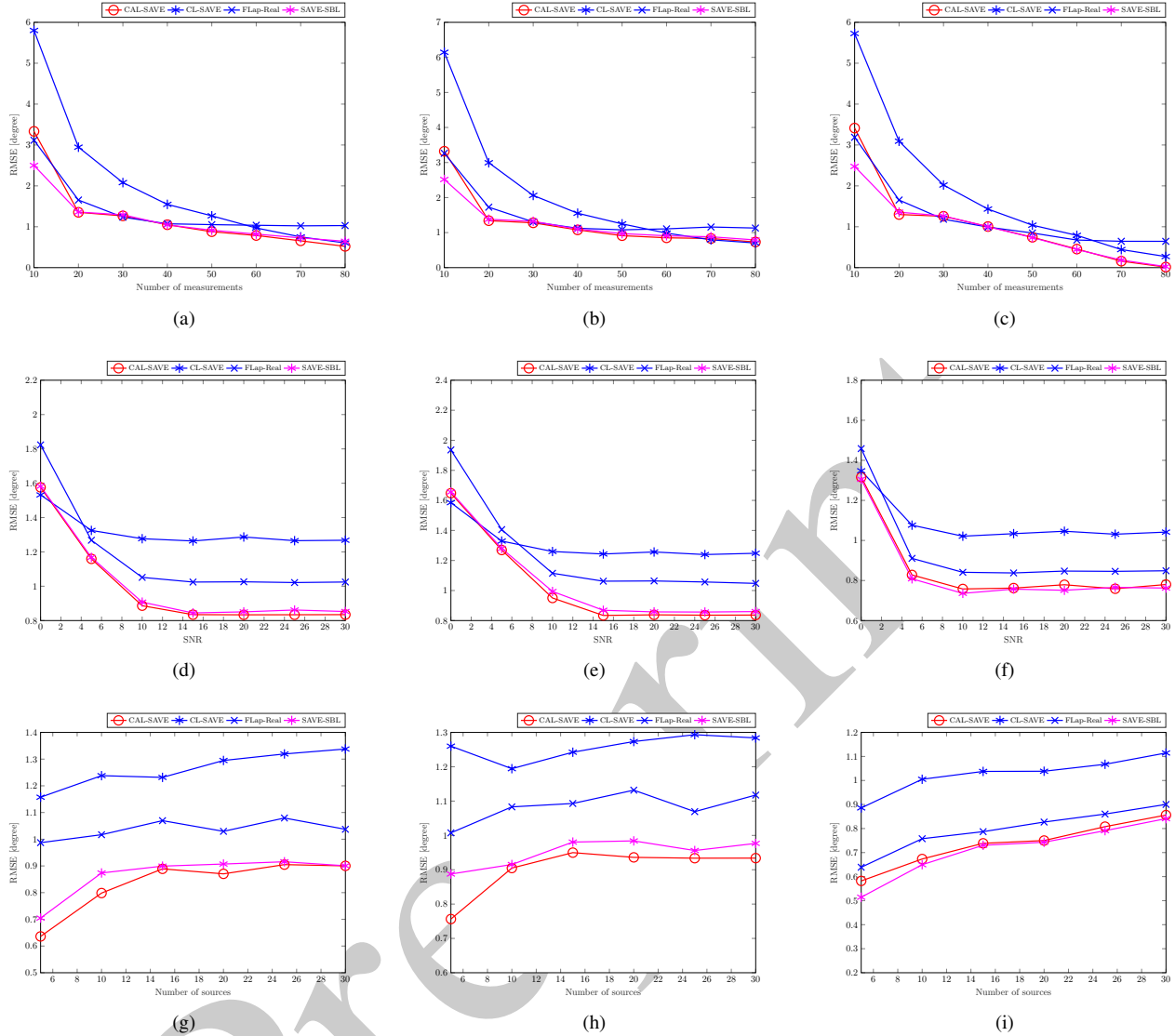


Fig. 8. Simulation results for DOA estimation. (a) RMSE versus the number of measurements for the Gaussian signal, (b) RMSE versus the number of measurements for the Laplace signal, (c) RMSE versus the number of measurements for the spike signal, (d) RMSE versus the sparsity for the Gaussian signal, (e) RMSE versus the sparsity for the Laplace signal, (f) RMSE versus the sparsity for the spike signal, (g) RMSE versus the SNR for the Gaussian signal, (h) RMSE versus the SNR for the Laplace signal, (i) RMSE versus the SNR for the spike signal.

perform better under high and known sparsity levels. However, similar to the SMV case, the proposed method achieves a better performance when the number of non-zero elements is greater than 25, even without prior knowledge of the sparsity level.

For the MMV case, both the ‘SBL-BF’ and ‘CSMUSIC’ methods perform better under either a small number of measurement vectors or a high and known sparsity level. However, the proposed method outperforms the others in most of the scenarios, even without prior knowledge of the sparsity level.

B. DOA estimation

In this subsection, the proposed method is applied to DOA estimation. We consider the case of DOA estimation with a uniform linear array. All K sources are located in front of the uniform linear array. The inner space of the adjacent array

elements is equal to half the wavelength. The target space is separated uniformly in the range from -90° to 90° with an interval of 0.5° , i.e., the number of grids is 361. The root mean square error is used to measure the estimation performance, which is defined as

$$\epsilon_{\text{RMSE}} = \frac{\sqrt{\sum_{n=1}^{N_{MC}} \sum_{k=1}^K (\hat{\theta}_k^n - \theta_k^n)^2}}{KN_{MC}}, \quad (42)$$

where θ_k^n denotes the truth DOA of the k th source at the n th MC experiment, whereas $\hat{\theta}_k^n$ is the estimation of θ_k^n , and N_{MC} is the total number of MC experiments.

1) Experimental setup:

- In the first experiment, the localization performance is tested for three types of signals under different lengths of measurements in the range from 10 to 80 with an interval of 10. The number of sources is set to 21. These

sources are uniformly located in the range from -10° to 10° . The angle between two adjacent sources is 1° . The SNR is set to 10 dB.

- In the second experiment, the performance is tested for different types of signals under different SNRs from 0 to 30 dB with an interval of 5 dB. The number of sources is set to 21. The number of measurements is set to 50.
- In the third experiment, the performance is tested for different types of signals under different numbers of sources from 5 to 30 with an interval of 5. The SNR is set to 10 dB. The number of measurements is set to 50.

2) *Performance analysis*: Figure 8a, Figure 8b and Figure 8c show the localization performance for three types of signals under different lengths of measurements, respectively. It can be seen that longer measurement vectors result in more accurate localization performances. The ‘CAL-SAVE’ and ‘SAVE-SBL’ methods perform the best in the various scenarios. Note that ‘CAL-SAVE’ outperforms the ‘SAVE-SBL’ method when the length of the measurement vector is larger than 20.

The performance of the different methods for the different types of signals under different SNRs is illustrated in Figure 8d, Figure 8e and Figure 8f. The localization accuracy increases as the SNR increases in the range from 0 to 20 dB. When the SNR is greater than 20 dB, the localization performance becomes stable. Similar to the first experiment, the proposed ‘CAL-SAVE’ method outperforms the other methods in most of the cases.

Figure 8g, Figure 8h and Figure 8i show the performance for the three types of signals under different numbers of sources. As can be seen from these figures, the proposed method performs the best with regard to the complex Gaussian signals and the complex Laplace signals.

VI. CONCLUSION

In this paper, we consider the complex sparse signal recovery problem. Motivated by the self-regularizing nature of the Bayesian framework and oracle properties of the adaptive LASSO, we build a hierarchical Bayesian model with adaptive Laplace priors to pursue the complex-value signal model. Moreover, we extend this Bayesian framework to the MMV case. The space alternative method is integrated into the proposed algorithm to avoid the use of the matrix inverse operation. The performance of the proposed method is tested using complex Gaussian random dictionaries for complex Gaussian signals, complex Laplace signals and complex spike signals, respectively. The experimental results show that the hierarchical Bayesian framework with adaptive Laplace priors improves the recovery performance for all of the types of signals studied, and especially for the complex Laplace signal. Furthermore, we have also demonstrated that the proposed method outperforms other state-of-the-art Bayesian methods for DOA estimation. The proposed hierarchical framework and algorithm are easy to implement and apply in complex signal recovery.

APPENDIX A

DERIVATION OF HIDDEN PARAMETERS FOR THE SMV CASE

1) *Update of $q_\lambda(\boldsymbol{\lambda})$* : The logarithmic approximate posterior of the variable λ_i is

$$\ln q(\lambda_i) = -\frac{1}{2} \ln \lambda_i - E_{q(\gamma_i)}(\gamma_i)\lambda_i - \lambda_i^{-1} E_{q(\mathbf{g})}(\mathbf{g}_i^* \mathbf{g}_i).$$

Note that the Gamma prior is not the conjugate prior of the complex Gaussian distribution with a known mean. Thus, we use a generalized inverse Gaussian distribution to represent the approximate posterior distribution of $q_\lambda(\boldsymbol{\lambda})$. The parameters of this generalized inverse Gaussian distribution are $p_\lambda = \frac{1}{2}$, $a = \frac{1}{2} E_{q(\gamma_i)}(\gamma_i)$ and $b = 2 E_{q(\mathbf{g})}(\mathbf{g}_i^* \mathbf{g}_i)$, where $E_{q(\mathbf{g})}(\mathbf{g}_i^* \mathbf{g}_i) = \mu_{g_i}^* \mu_{g_i} + \Sigma_{g_{ii}}$, μ_{g_i} and $\Sigma_{g_{ii}}$ are the i th element of the vector $\boldsymbol{\mu}_g$ and the i th diagonal element of the matrix $\boldsymbol{\Sigma}_g$. Therefore, the means of λ_i and λ_i^{-1} are

$$E_{q(\lambda_i)}(\lambda_i) = \frac{\sqrt{b} K_{\frac{3}{2}}(\sqrt{ab})}{\sqrt{a} K_{\frac{1}{2}}(\sqrt{ab})} = \frac{\sqrt{b}}{\sqrt{a}} + \frac{1}{a}, \quad (43)$$

$$E_{q(\lambda_i)}(\lambda_i^{-1}) = \frac{\sqrt{a} K_{\frac{3}{2}}(\sqrt{ab})}{\sqrt{b} K_{\frac{1}{2}}(\sqrt{ab})} - \frac{2p}{b} = \frac{\sqrt{a}}{\sqrt{b}}. \quad (44)$$

2) *Update of $q(\gamma)$* : The approximate posterior of γ_i is

$$\ln q(\gamma_i) = \left(c + \frac{1}{2}\right) \ln \gamma_i - \left(\frac{1}{4} E_{q(\lambda_i)}(\lambda_i) + d\right) \gamma_i, \quad (45)$$

which indicate that γ_i follows a Gamma distribution with the parameters $\alpha_\gamma = \frac{3}{2} + c$ and $\beta_\gamma = \frac{1}{4} E_{q(\lambda_i)}(\lambda_i) + d$. Therefore, the mean of γ_i is

$$E_{q(\gamma_i)} = \frac{\alpha_\gamma}{\beta_\gamma}. \quad (46)$$

3) *Update of $q(\rho)$* : The approximate posterior of ρ is

$$\ln q(\rho) = (a + M - 1) \ln \rho - \left(E_{q(\mathbf{g})}(\|\mathbf{x} - \mathbf{A}\mathbf{g}\|^2) + b\right) \rho,$$

which indicates that ρ follows a gamma distribution with the parameters $\alpha_\rho = M + a$ and $\beta_\rho = E_{q(\mathbf{g})}(\|\mathbf{x} - \mathbf{A}\mathbf{g}\|^2) + b$, where

$$E_{q(\mathbf{g})}(\|\mathbf{x} - \mathbf{A}\mathbf{g}\|^2) = \|\mathbf{x} - \mathbf{A} E_{q(\mathbf{g})}(\mathbf{g})\|^2 + \text{tr}(\boldsymbol{\Sigma}_g \mathbf{A}^H \mathbf{A}).$$

Thus, the mean of ρ is

$$E_{q(\rho)} = \frac{\alpha_\rho}{\beta_\rho}. \quad (47)$$

APPENDIX B

DERIVATION OF HIDDEN PARAMETERS FOR THE MMV CASE

1) *Update of $q(\boldsymbol{\lambda})$* : Similar to the SMV case, the approximate posterior of λ_i can be written as

$$\begin{aligned} \ln q(\lambda_i) &= E_{q(\boldsymbol{\theta} \setminus \lambda_i)}(p(\mathbf{X}, \boldsymbol{\theta})), \\ &= -\frac{1}{2} \ln \lambda_i - \frac{1}{4} E_{q(\gamma_i)}(\gamma_i)\lambda_i - \lambda_i^{-1} E_{q(\mathbf{g}_i)}\left(\text{tr}(\mathbf{g}_i^H \mathbf{g}_i)\right) + c_\lambda, \end{aligned}$$

which indicates that λ_i follows an inverse Gaussian distribution with the parameters $p = \frac{1}{2}$, $a = \frac{1}{2} E_{q(\gamma_i)}(\gamma_i)$ and $b =$

$2\mathbb{E}_{q(g_i)}\left(\text{tr}(\mathbf{g}_i^H \mathbf{g}_i)\right)$, where $\mathbb{E}_{q(g_i)}\left(\text{tr}(\mathbf{g}_i^H \mathbf{g}_i)\right) = \boldsymbol{\mu}_i^H \boldsymbol{\mu}_i + \sigma_i$. Thus, we obtain

$$\mathbb{E}_{q(\lambda_i)}(\lambda_i) = \frac{\sqrt{b}}{\sqrt{a}} + \frac{1}{a}. \quad (48)$$

$$\mathbb{E}_{q(\lambda_i)}(\lambda_i^{-1}) = \frac{\sqrt{a}}{\sqrt{b}}. \quad (49)$$

2) *Update of $q(\gamma)$* : The (37) leads to a Gamma distribution for the approximate distribution of γ_i , that is

$$\begin{aligned} \ln q(\gamma_i) &= \mathbb{E}_{q(\boldsymbol{\theta} \setminus \gamma_i)}(p(\mathbf{X}, \boldsymbol{\theta})), \\ &= \left(L + c - \frac{1}{2}\right) \ln \gamma_i - \left(\frac{1}{4}\mathbb{E}_{q(\lambda_i)}(\lambda_i) + d\right) \gamma_i + c_\gamma, \end{aligned}$$

with the parameters $\alpha_\gamma = L + c + \frac{1}{2}$ and $\beta_\gamma = \frac{1}{4}\mathbb{E}_{q(\lambda_i)}(\lambda_i) + d$. Thus, the mean of γ_i for the MMV case is

$$\mathbb{E}_{q(\gamma_i)}(\gamma_i) = \frac{\alpha_\gamma}{\beta_\gamma}. \quad (50)$$

3) *Update of $q(\rho)$* : Similarly, the approximate distribution of ρ is

$$\begin{aligned} \ln q(\rho) &= \mathbb{E}_{q(\boldsymbol{\theta} \setminus \rho)}(p(\mathbf{X}, \boldsymbol{\theta})), \\ &= (LM + a - 1) \ln \rho - \left(\mathbb{E}_{q(\mathbf{G})}\left(\|\mathbf{X} - \mathbf{A}\mathbf{G}\|_f^2\right) + b\right) \rho, \end{aligned}$$

which indicates that ρ follows a Gamma distribution with the parameters as follows:

$$\alpha_\rho = LM + a, \beta_\rho = \mathbb{E}_{q(\mathbf{G})}\left(\|\mathbf{X} - \mathbf{A}\mathbf{G}\|_f^2\right) + b,$$

where

$$\mathbb{E}_{q(\mathbf{G})}(\|\mathbf{X} - \mathbf{A}\mathbf{G}\|_f^2) = \|\mathbf{X} - \mathbf{A}\mathbb{E}_{q(\mathbf{G})}(\mathbf{G})\|_f^2 + \text{tr}(\boldsymbol{\Sigma}\mathbf{A}^H\mathbf{A}).$$

Thus, we have

$$\mathbb{E}_{q(\rho)}(\rho) = \frac{\alpha_\rho}{\beta_\rho}. \quad (51)$$

REFERENCES

- [1] I. F. Gorodnitsky, J. S. George, and B. D. Rao, "Neuromagnetic source imaging with FOCUSS: a recursive weighted minimum norm algorithm," *Electroencephalography and Clinical Neurophysiology*, vol. 95, no. 4, pp. 231–251, oct 1995.
- [2] Y. C. Eldar and G. Kutyniok, Eds., *Compressed Sensing*. Cambridge University Press, 2009.
- [3] I. Gorodnitsky and B. Rao, "Sparse signal reconstruction from limited data using FOCUSS: a re-weighted minimum norm algorithm," *IEEE Transactions on Signal Processing*, vol. 45, no. 3, pp. 600–616, mar 1997.
- [4] M. F. Duarte and R. G. Baraniuk, "Spectral compressive sensing," *Applied and Computational Harmonic Analysis*, vol. 35, no. 1, pp. 111–129, jul 2013.
- [5] Z. Yang, J. Li, P. Stoica, and L. Xie, "Sparse methods for direction-of-arrival estimation," in *Academic Press Library in Signal Processing*, C. Rama and T. Sergios, Eds., 2018, vol. 7, pp. 509–581.
- [6] M. Carlin, P. Rocca, G. Oliveri, F. Viani, and A. Massa, "Directions-of-arrival estimation through bayesian compressive sensing strategies," *IEEE Transactions on Antennas and Propagation*, vol. 61, no. 7, pp. 3828–3838, jul 2013.
- [7] H. Bai, M. F. Duarte, and R. Janaswamy, "Direction of arrival estimation for complex sources through l_1 norm sparse bayesian learning," *IEEE Signal Processing Letters*, vol. 26, no. 5, pp. 765–769, may 2019.
- [8] R. Tibshirani, "Regression shrinkage and selection via the lasso," *Journal of the Royal Statistical Society. Series B (Methodological)*, vol. 58, no. 1, pp. 267–288, 1996.
- [9] A. Maleki, L. Anitori, Z. Yang, and R. G. Baraniuk, "Asymptotic analysis of complex LASSO via complex approximate message passing (CAMP)," *IEEE Transactions on Information Theory*, vol. 59, no. 7, pp. 4290–4308, jul 2013.
- [10] H. Zou, "The adaptive lasso and its oracle properties," *Journal of the American Statistical Association*, vol. 101, no. 476, pp. 1418–1429, dec 2006.
- [11] E. J. Candès, M. B. Wakin, and S. P. Boyd, "Enhancing sparsity by reweighted ℓ_1 minimization," *Journal of Fourier Analysis and Applications*, vol. 14, no. 5–6, pp. 877–905, oct 2008.
- [12] R. J. Tibshirani and J. Taylor, "The solution path of the generalized lasso," *The Annals of Statistics*, vol. 39, no. 3, pp. 1335–1371, jun 2011.
- [13] J. Fan and L. R., "Variable selection via nonconcave penalized likelihood and its oracle properties," *Journal of the American Statistical Association*, vol. 96, pp. 1348–1360, 2001.
- [14] J. Tropp and A. Gilbert, "Signal recovery from random measurements via orthogonal matching pursuit," *IEEE Transactions on Information Theory*, vol. 53, no. 12, pp. 4655–4666, Dec 2007.
- [15] D. L. Donoho, Y. Tsaig, I. Drori, and J.-L. Starck, "Sparse solution of underdetermined systems of linear equations by stagewise orthogonal matching pursuit," *IEEE Transactions on Information Theory*, vol. 58, no. 2, pp. 1094–1121, feb 2012.
- [16] T. Blumensath and M. Davies, "Gradient pursuits," *IEEE Transactions on Signal Processing*, vol. 56, no. 6, pp. 2370–2382, Jun 2008.
- [17] M. G. Christensen and S. H. Jensen, "The cyclic matching pursuit and its application to audio modeling and coding," in *2007 Conference Record of the Forty-First Asilomar Conference on Signals, Systems and Computers*. IEEE, nov 2007.
- [18] W. Dai and O. Milenkovic, "Subspace pursuit for compressive sensing signal reconstruction," *IEEE Transactions on Information Theory*, vol. 55, no. 5, pp. 2230–2249, may 2009.
- [19] M. E. Tipping and A. Smola, "Sparse bayesian learning and the relevance vector machine," *The Journal of Machine Learning Research*, vol. 59, no. 1, pp. 211–244, 2001.
- [20] S. Babacan, R. Molina, and A. Katsaggelos, "Bayesian compressive sensing using laplace priors," *IEEE Transactions on Image Processing*, vol. 19, no. 1, pp. 53–63, jan 2010.
- [21] K. E. Themelis, A. A. Rontogiannis, and K. D. Koutroumbas, "A novel hierarchical Bayesian approach for sparse semisupervised hyperspectral unmixing," *IEEE Transactions on signal processing*, vol. 60, no. 2, pp. 585–599, Feb 2012.
- [22] C. Leng, M.-N. Tran, and D. Nott, "Bayesian adaptive Lasso," *Annals of the Institute of Statistical Mathematics*, vol. 66, pp. 221–244, 2014.
- [23] M. E. Tipping, A. Faul, J. J. T. Avenue, and J. J. T. Avenue, "Fast marginal likelihood maximisation for sparse bayesian models," in *Proceedings of the Ninth International Workshop on Artificial Intelligence and Statistics*, 2003, pp. 3–6.
- [24] Y. Zheng, A. Fraysse, and T. Rodet, "Efficient variational bayesian approximation method based on subspace optimization," *IEEE Transactions on Image Processing*, vol. 24, no. 2, pp. 681–693, feb 2015.
- [25] C. K. Thomas and D. Slock, "SAVE - space alternating variational estimation for sparse bayesian learning," in *2018 IEEE Data Science Workshop (DSW)*. IEEE, jun 2018.
- [26] P. Gerstoft, C. F. Mecklenbrauker, A. Xenaki, and S. Nannuru, "Multisnapshot sparse bayesian learning for DOA," *IEEE Signal Processing Letters*, vol. 23, no. 10, pp. 1469–1473, oct 2016.
- [27] M. A. T. Figueredo, "Adaptive sparseness for supervised Bayesian learning," *IEEE Transactions on pattern analysis, machine intelligence*, vol. 25, no. 9, pp. 1150–1159, 2003.
- [28] M. Novey, T. Adali, and A. Roy, "A complex generalized gaussian distribution—characterization, generation, and estimation," *IEEE Transactions on Signal Processing*, vol. 58, no. 3, pp. 1427–1433, mar 2010.
- [29] D. G. Tzikas, A. C. Likas, and N. P. Galatsanos, "The variational approximation for bayesian inference," *IEEE Signal Processing Magazine*, vol. 25, no. 6, pp. 131–146, nov 2008.
- [30] S. Cotter, B. Rao, K. Engan, and K. Kreutz-Delgado, "Sparse solutions to linear inverse problems with multiple measurement vectors," *IEEE Transactions on Signal Processing*, vol. 53, no. 7, pp. 2477–2488, jul 2005.
- [31] A. Xenaki, J. B. Boldt, and M. G. Christensen, "Sound source localization and speech enhancement with sparse bayesian learning beamforming," *The Journal of the Acoustical Society of America*, vol. 143, no. 6, pp. 3912–3921, jun 2018.
- [32] C. M. Bishop, *Pattern Recognition and Machine Learning*. Springer, 2006.